Monthly Notices of the ROYAL ASTRONOMICAL SOCIETY

MNRAS **521,** L11–L16 (2023) https://doi.org/10.1093/mnrasl/slad014
Advance Access publication 2023 February 6

# An empirical relation to estimate host galaxy stellar light from AGN spectra

Priyanka Jalan,[1,2] Suvendu Rakshit,[2]★ Jong-Jak Woo,[3] Jari Kotilainen[4] and C. S. Stalin[5]

[1] *Center for Theoretical Physics of the Polish Academy of Sciences, Al. Lotników 32/46, PL-02-668 Warsaw, Poland*
[2] *Aryabhatta Research Institute of Observational Sciences (ARIES), Manora Peak, Nainital, 263002, India*
[3] *Astronomy Program, Department of Physics and Astronomy, Seoul National University, Seoul 151-742, Republic of Korea*
[4] *Finnish Centre for Astronomy with ESO (FINCA), FI-20014 University of Turku, Finland*
[5] *Indian Institute of Astrophysics, Block II, Koramangala, Bangalore-560034, India*

Accepted 2023 February 2. Received 2023 February 2; in original form 2022 October 3

## ABSTRACT

Measurement of black hole mass for low-$z$ ($z \leq 0.8$) Active Galactic Nuclei (AGNs) is difficult due to the strong contribution from host galaxy stellar light necessitating detailed spectral decomposition to estimate the AGN luminosity. Here, we present an empirical relation to estimate host galaxy stellar luminosity from the optical spectra of AGNs at $z \leq 0.8$. The spectral data were selected from the fourteenth data release of the Sloan Digital Sky Survey (SDSS-DR14) quasar catalogue having a signal-to-noise ratio at 5100 Å ($\mathrm{SNR}_{5100}$) >10 containing 11 415 quasars. The median total luminosity (log ($L_{\mathrm{total}}$/[erg s$^{-1}$])), stellar luminosity (log ($L_{\mathrm{star}}$/[erg s$^{-1}$])), and AGN continuum luminosity ((log $L_{\mathrm{cont}}$/[erg s$^{-1}$])) in our sample are 44.52, 44.06, and 44.30, respectively. We fit the AGN power-law continuum, host galaxy, and iron blend contribution, simultaneously over the entire available spectrum. We found the host galaxy fraction to anticorrelate with continuum luminosity and can be well-represented by a polynomial function, which can be used to correct the stellar light contribution from AGN spectra. We also found anticorrelation between host galaxy fraction and iron strength, Eddington ratio, and redshift. The empirical relation gives comparable results of host-fraction with the image decomposition method.

**Key words:** methods: data analysis – galaxies: active – methods: statistical.

## 1 INTRODUCTION

Active galactic nuclei (AGNs) are powered by the accretion of matter on to a supermassive black hole ($>10^5\,\mathrm{M}_\odot$) with luminosity ranging from $10^{44}$–$10^{48}$ erg s$^{-1}$. Previous studies suggest that nearly all massive galaxies host supermassive black holes (SMBHs), and the properties of these SMBHs show correlations with the properties of the host galaxy, indicating a strong connection between them (see Kormendy & Ho 2013 for a review). Massive black holes may originate before the era that marks the peak of galaxy formation (at $z \sim 2$), as evident by the history of star formation in bright galaxies (Madau & Dickinson 2014). As a result, it gives credence to theoretical arguments that spheroid formation and the growth of SMBHs are closely linked and the associated extensive energetic outflows from AGN may have a significant correlation with physical processes in the host galaxy.

To understand this relation between black holes and their host galaxy, it is crucial to emphasize their spectral decomposition (Greene & Ho 2005; Shen et al. 2011; Bongiorno et al. 2014; Varisco et al. 2018; Rakshit, Stalin & Kotilainen 2020). This is especially important at low-$z$ in optical wavelengths where the contamination by their host galaxy is significant. The advent of large surveys such as the Sloan Digital Sky Survey (SDSS) and Dark Energy Spectroscopic Instrument (DESI), which capture millions of such AGNs, motivates us to find an empirical relation between fraction of luminosity from the black hole and their host galaxy, that can be used for further studies. For example, black hole masses in AGNs are mostly calculated using the virial relation given by the reverberation mapping study, which uses the luminosity of the continuum to find the size of the broad line region (or radius-luminosity relation) (e.g. Shen et al. 2011; Rakshit et al. 2020). Non-removal of the host galaxy may lead to an overestimation of the luminosity and hence the black hole mass.

Various methods have been developed to decompose the host galaxy contribution correctly and to maximize the use of archival data. Recent studies by Rakshit et al. (2020, hereafter R20) used SDSS-DR14 quasar sample and decomposed host galaxy and quasar contribution using principal component analysis (PCA). Similarly, Calderone et al. (2017, hereafter C17) and Varisco et al. (2018) used SDSS-DR10 sample at $z < 0.6$ and $z < 0.8$, respectively to account for this host galaxy contamination. C17 developed an automated software package, QSFIT[1] that decomposes the spectrum into the host galaxy and AGN continuum, the Balmer continuum emission, optical and ultraviolet iron blended complex, and emission lines. They have used a power-law model for AGN and an elliptical galaxy template for the host galaxy. Similarly, Shen et al. (2011) estimated the host galaxy

★ E-mail: priyajalan14@gmail.com (PJ); suvenduat@gmail.com (SR)

[1] https://github.com/gcalderone/qsfit

contamination for $z \leq 0.5$ quasars using stacked spectra assuming that the highest luminosity bin (log ($L_{\rm cont}$/[erg s$^{-1}$]) = 45.5) is not affected by host galaxy contamination. Berk et al. (2006) separated the host galaxy using the PCA method from the broad line AGN for 4666 spectra from SDSS at $z \leq 0.75$ and found dependence on various parameters such as signal-to-noise ratio (SNR) and host galaxy class.

Detailed spectral decomposition is necessary to remove the host contamination, however, high SNR spectra along with clear detection of absorption lines are required for such spectral decomposition. Unfortunately, a majority of the spectra obtained in large surveys do not have high SNR. In this paper, we carried out a detailed spectral decomposition for $z\leq$ 0.8 AGNs in the SDSS-DR14 (Pâris et al. 2018) catalogue by performing an independent fit of each AGN spectrum to obtain an empirical relation between host galaxy fraction and AGN continuum luminosity that can be used to estimate the host-fraction for low-SNR spectra where detailed spectral decomposition is difficult to perform. The paper is organized as follows: In Section 2, we discuss the spectral data used and its various components. In Section 3, we detailed our results followed by a comparison with previous studies. We also analysed the variation of host galaxy fraction with redshift, SNR and other AGN parameters. Finally, we conclude our work in Section 4. Throughout, we used a flat background cosmology with $\Omega_m = 0.3$, $\Omega_\lambda = 0.7$, and $H_o = 70$ km s$^{-1}$ Mpc $^{-1}$.

## 2 DATA AND SPECTRAL FITTING

We used the complete compilation of the SDSS-DR14 quasar catalogue and more sophisticated parameter measurements from R20. We limited the analysis to $z \leq 0.8$ sources for which SDSS covers $\lambda < 5000$ Å (rest frame) providing a better constraint to the host galaxy contribution, resulting in 55 427 sources. The host galaxy fraction (hf $\equiv L_{\rm star}/L_{\rm total}$) cannot be precisely measured for a very low-SNR spectrum therefore, we limited the sample with SNR at 5100 Å ($\mathrm{SNR}_{5100}$) > 10. This includes 11 415 spectroscopically confirmed quasars with a median $\mathrm{SNR}_{5100}$ of ∼15.

Each observed spectrum was corrected for Galactic extinction using the Schlegel, Finkbeiner & Davis (1998) extinction map and the Milky Way extinction law with $R_V = 3.1$ from Cardelli, Clayton & Mathis (1989). Then the spectra were converted to their respective rest-frame (based on their redshift). After masking the strong emission lines, we modelled each spectrum using a combination of starlight from the host galaxy, AGN power-law and iron blends with their contribution varying from source to source, as discussed below.

**Star light**: The photons from the stars present in the host galaxy contribute to the total AGN spectrum, especially at low−$z$ in optical wavelengths. In order to model the stellar contribution, we used the stellar template from the Indo-US spectral library (Valdes et al. 2008), which has been previously used by various authors (Rakshit & Woo 2018). It contains seven spectra of G- and K-type giant stars of various temperatures with a resolution of 1.35 Å and covering the wavelength range of 3650–9200 Å. The templates were broadened by a Gaussian kernel with line width as a free parameter along with the velocity shift as another free parameter. The weights were optimized for each stellar template.

**AGN continuum:** The AGN contribution is simply a power-law of the form

$$L_\lambda = A \times (\lambda/5100)^B, \qquad (1)$$

where A is the luminosity density at 5100 Å or the normalization parameter and B is the spectral slope. The line-free region of the entire spectral range is used for this continuum fitting. Even for large spectral coverage, we assumed a single power-law, however, a broken power-law can also be modelled. However, in the sources that have star-light contributions similar to or higher than the AGN contribution the slope degenerates with the star-light and hence the broken power-law cannot be well constrained.

**Iron lines:** We considered the spectral range of 4000–6000 Å to perform the spectral fitting and modelled the optical Fe II emission using the Fe II templates constructed by Kovačević, Popović & Dimitrijević (2010). Previous studies found that this template provides a better fit for the Fe II emission in AGN (Barth et al. 2015). The UV component of the Fe II emission ranging from 1250–3090 Å is not relevant in the present decomposition i.e. >3650 Å. The Kovačević et al. (2010) Fe II template consists of five different templates representing different groups of multiplet, therefore, normalization of each template was needed. The Fe II template spectra were convolved using a Gaussian broadening kernel as done for the stellar template. The width and the shift of all five templates were kept the same for a given spectral fit. The total continuum is a combination of the host galaxy, AGN power-law, and Fe II emission.

**Emission lines:** After the subtraction of the total continuum from the spectrum the emission lines (broad and narrow) were fitted. The emission line complex is fitted over the spectral range of 4600–5050 Å. We fitted the broad component using a 6th order Gaussian Hermite function and each narrow component using a single Gaussian. The O III doublets were fitted using double Gaussian. Using the best-fit model, we extracted the parameters such as emission line flux and full width at half-maximum (FWHM) which is used to calculate the black hole mass and Eddington ratio (using Rakshit & Woo 2018).

The best-fit model was found by performing a non-linear Levenberg–Marquardt least-squares minimization using MPFIT3 (Markwardt 2009) code in IDL. This allowed us to properly decompose different model components estimating host galaxy fraction and the host-subtracted continuum luminosity at 5100 Å. Fig. 1 presents an overview of the results of our continuum fitting procedures. The top and bottom panel shows a spectrum with high SNR (∼34) at $z = 0.07$ and SNR (∼11) at $z = 0.48$, with ∼ 76 per cent and ∼ 54 per cent host contribution, respectively. Individual decomposed components are also shown.

## 3 RESULTS

### 3.1 Comparison with previous studies

We compare our results of host galaxy fraction estimate with that obtained by C17 and R20, enlisting the similarities and dissimilarities. R20 first decomposed the spectrum using 5 PCA components for the galaxy and 20 PCA components for quasars. After subtracting the galaxy contribution, they fitted the residual with a power-law continuum and iron template masking the emission lines. On the other hand, C17 fitted different components of the continuum and emission lines simultaneously where the host galaxy is represented by a single elliptical galaxy template of Mannucci et al. (2001) with the only free parameter being the normalization factor.

For the AGN contribution, R20 uses a similar power-law as mentioned in equation (1). However, unlike our varying spectral slope, C17 assumes a fixed value of $B = -1.7$ for low-redshift ($z \leq 0.6$) AGNs due to the difficulty of separating stellar and non-stellar

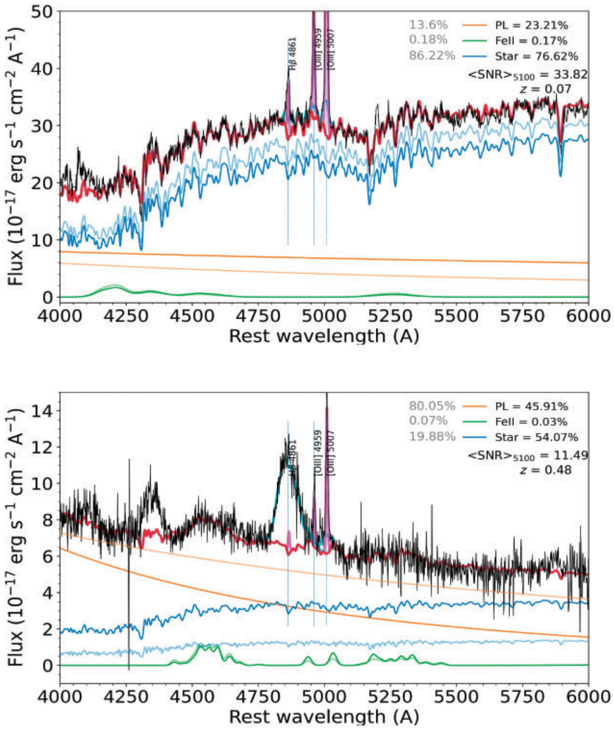


**Figure 1.** The plot shows two spectra with their individual components. The AGN continuum, iron continuum, and host galaxy fraction are shown in orange, green, and blue colour, with contributions mentioned as PL, Fe II, and star, respectively. The fainter colour shows the spectral decomposition for the constant spectral slope of −1.7 (see text in Section 3.1). The top panel shows an example of high galaxy contribution with higher SNR ∼34 at $z \sim 0.07$ and the bottom panel shows an example of ∼ 54 per cent galaxy contribution at lower SNR ∼11 at $z \sim 0.48$. The plot also shows broad (cyan) and narrow (fuchsia) components of the emission lines.

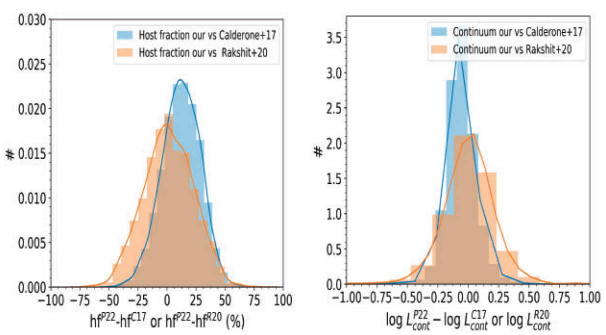


**Figure 2.** Comparing host galaxy fraction (left) and continuum luminosity (right) calculated in this work with C17 and R20 at 5100 Å. Histograms of their differences are shown.

components in AGNs closer than $z \sim 0.7$. Similar to C17, we also tested our spectral decomposition for the spectra with a constant spectral slope. We show this spectral decomposition in fainter colour in Fig. 1.

We compare the host galaxy fraction percentage calculated in this work with that obtained by C17 and R20 for the common sources in Fig. 2. The mean difference of the host galaxy fraction between this work and R20 is 1.51 ± 21.34 per cent while this work and C17 is 11.92 ± 16.64 per cent. This suggests our host galaxy fraction is more consistent with R20 than C17 measurements although with a larger scatter with R20 compared to C17. A large fraction of sources with host galaxy fraction ∼30 per cent as estimated in this work have almost nil host contamination in C17. The difference in the host contribution measurement by different authors could be mainly due to the use of different host galaxy decomposition methods. Since C17 assumed the host galaxy to be an elliptical galaxy and low-luminous AGNs are found to be hosted in spiral galaxies, such an assumption could underestimate the host galaxy flux measurement, especially in low-luminosity AGNs (Crenshaw, Kraemer & Gabel 2003; Olguín-Iglesias, Kotilainen & Chavushyan 2019; Gkini et al. 2021, and references therein). The right-hand panel of Fig. 2 shows the consistency of the continuum luminosity with R20 and a slight difference with respect to estimates by C17. Furthermore, we checked if using a fixed spectral slope by C17 could be the reason, and we found the mean difference of the host galaxy fraction of this work and C17 reduces to 6.37 ± 23.77 per cent, if the spectral slope fixed to $B = -1.7$. On the other hand, R20 uses the PCA method which assumes that each spectrum can be defined by combining two independent sets of eigen-spectra from the pure galaxy and the pure quasar samples. Moreover, only if the host galaxy fraction in the wavelength range of 4160–4210 Å is larger than 10 per cent the decomposition is considered effective whereas we apply no such constraint.

### 3.2 Host galaxy fraction versus continuum luminosity

The correlation between the host galaxy fraction and the luminosity at 5100 Å is shown in Fig. 3. The median 5100 Å total luminosity (log ($L_{\rm total}$/[erg s$^{-1}$])), stellar luminosity (log ($L_{\rm star}$/[erg s$^{-1}$])), and AGN continuum luminosity (log ($L_{\rm cont}$/[erg s$^{-1}$])) in our sample are 44.524, 44.062, and 44.301, respectively. All the luminosity (i.e, $L_{\rm star}$, $L_{\rm cont}$, and $L_{\rm total}$) estimates are found to be increasing with the redshift, with varying slopes. This is contributed by two factors: (i) There is a bias in selecting more luminous quasars at higher−$z$ due to flux-limited observations and (ii) more host galaxy light will be available in the 3 arcsec SDSS aperture for higher−$z$ targets because of the smaller angular size of the host galaxy. However, the continuum luminosity is found to have a steeper slope with redshift as compared to the stellar luminosity.

It is evident from Fig. 3 that the host galaxy luminosity fraction decreases as the continuum luminosity increases. This is clear from the (median) binned data plot which shows a decreasing trend. The host galaxy luminosity fraction is dominant with >50 per cent for the continuum luminosity $<10^{43.7}$ erg s$^{-1}$. As expected, at a given $L_{\rm cont}$, there is a large dispersion in the host galaxy fraction. This is because, for a given $L_{\rm cont}$ there would be sources with a distribution of Eddington ratios, which means sources with a range of black hole mass (or a range of $L_{\rm star}$ due to the correlation between black hole mass and stellar mass) leading to a large distribution of host-fraction.

In order to find a mathematical relation between the host galaxy fraction with the total AGN luminosity, we fitted the binned data in the top panel of Fig. 3 using a third-order polynomial and found

$$y = (42.01 \pm 1.15) + (-20.53 \pm 1.47)x + (9.34 \pm 2.45)x^2 + (-3.88 \pm 1.33)x^3, \quad (2)$$

where $x = \log L_{\rm total} - 44$.

We estimate the host-fraction of individual objects based on the above empirical relation and compare them with the direct measurement from model fitting. The mean difference of host-fraction estimated between the two methods is ∼0 per cent with a dispersion of ∼15 per cent. As mentioned above, we also calculated

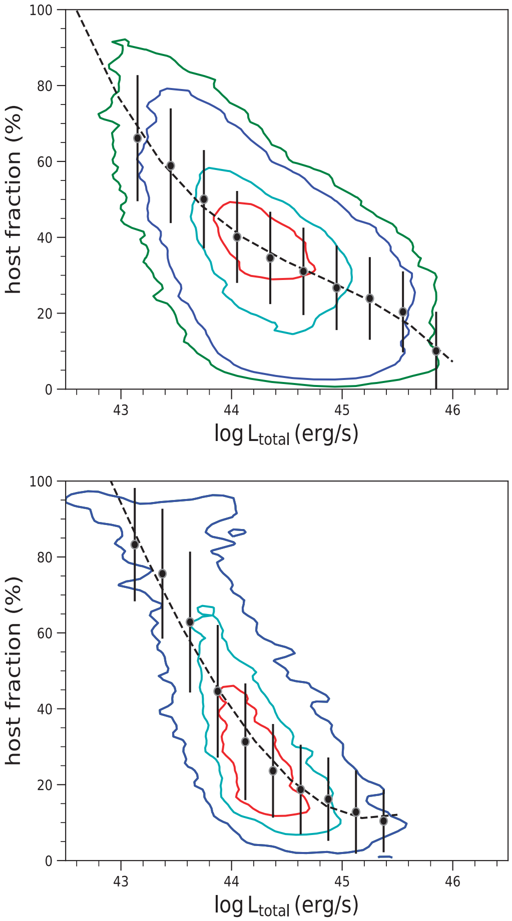


**Figure 3.** Top panel: The density contours represent the host luminosity fraction to that of total luminosity at 5100 Å versus continuum luminosity at 5100 Å in this work. The 40 percentile, $1\sigma$, $2\sigma$, and $3\sigma$ contours are shown. The points represent the median of the sample in each luminosity bin with error-bars showing the standard deviation in the bin. The best-fit polynomial fit of the binned data is shown by the dashed line. Bottom panel: Same as the top panel but for spectral slope fixed to −1.7.

the host galaxy fraction by fixing the spectral slope to be −1.7, and the modified host galaxy fraction versus total luminosity is shown in the bottom panel of Fig. 3. The modified equation for fixed spectral slope is

$$y = (39.87 \pm 1.96) + (-42.52 \pm 3.08)x + (13.39 \pm 3.93)x^2 + (1.73 \pm 3.52)x^3. \quad (3)$$

### 3.3 Host galaxy fraction with redshift and SNR

In Fig. 4 (left-hand panel), we show the host galaxy fraction as a function of redshift. We found that the host galaxy fraction percentage reduces as we go to higher redshifts, which is expected. With the increasing redshift, the continuum luminosity is found to increase (as shown by the colour bar), and thus the host fraction decreases. Spectral decomposition is sensitive to the SNR, and higher reliability of decomposition is expected for higher SNR spectra. In order to study the dependence of SNR on the host galaxy fraction, we used a subsample of high SNR data which have a host galaxy fraction ($hf_{ori}$) >20 per cent. We calculated the host galaxy fraction (hf) for spectra after degrading their SNR. For this, we first multiplied a factor of 2 to 10 by the original flux error for each high SNR spectra. We then added to the original flux spectra a Gaussian random deviation of zero mean and standard deviation given by the new flux errors. We then performed the spectral decomposition from these mock spectra as done for the original spectra and calculated the host galaxy fraction. We evaluated the ratio of $hf/hf_{ori}$ as plotted in the right-hand panel of Fig. 4, here the red squares show the median values. As evident from the plot, the scatter at lower SNR <10 is larger although the median value is consistent with unity. Therefore, the host galaxy fraction estimates are reliable only for SNR >10. This justifies the use of spectra having SNR >10 for this work.

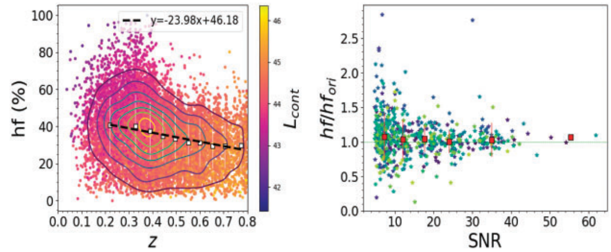


**Figure 4.** Fraction of host luminosity as compared to the total luminosity at $\lambda \sim 5100$ Å as a function of redshift (left-hand panel) and SNR at 5100 Å (right-hand panel). Multiple objects are shown with stars in different colours. The red squares represent the median in each bin.

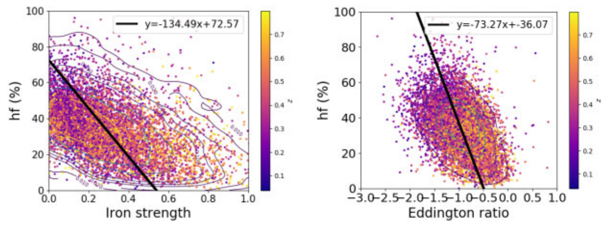


**Figure 5.** The plot shows host luminosity as compared to the total luminosity at $\lambda \sim 5100$ Å versus iron strength (left-hand panel) and Eddington ratio (right-hand panel), respectively. The colour bar represents the redshift. The black line represents the robust linear regression fitting using BCES.

### 3.4 Host galaxy fraction and AGN parameters

To study the dependency of host luminosity fraction with AGN parameters, we estimated black hole mass and Eddington ratio. The black hole mass was calculated using the virial relation from the single-epoch spectrum based on the FWHM of the H$\beta$ emission line and AGN luminosity at 5100 A using the relation given by Woo et al. (2015). The Eddington ratio was estimated by the ratio of Bolometric to Eddington luminosity, where the latter was calculated from the black hole mass (Rakshit & Woo 2018). Previous studies found an anticorrelation between iron strength and [O III] while a strong positive correlation between iron strength and Eddington ratio (e.g. Boroson & Green 1992; Rakshit et al. 2017). To study the correlation between host-fraction and iron strength, we estimated iron strength using the ratio of optical Fe II flux of the Fe II multiplets integrated over the wavelength range of 4434–4684 Å to H$\beta$ broad component. In the left-hand panel of Fig. 5, we show the host galaxy fraction versus the iron strength. We found host galaxy fraction is anticorrelated with the iron strength. Since high accreting sources are strong Fe II emitters, therefore, the host galaxy fraction should be anticorrelated with the Eddington ratio also. As expected, the host galaxy fraction reduces with the increment in the Eddington ratio as shown in the right-hand panel of Fig. 5.

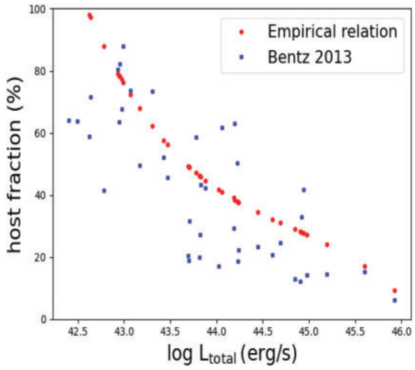


**Figure 6.** The plot shows the host fraction values calculated by Bentz et al. (2013) (blue squares) using the surface brightness decomposition and using the empirical relation derived in this work in equation (2) (red circle) as a function of total luminosity.

### 3.5 Impact of limited stellar templates

In this study, we have not included OB stellar templates in our stellar template list (e.g. see Section 2) due to their strong blue (along with the lack of absorption features in the wavelength range of 4000–6000 Å) spectra that is indistinguishable from the AGN power-law continuum. This leads to a high degeneracy in the model decomposition. Therefore, we can expect a systemic underestimation of the host fraction, especially, for AGNs with a high fraction of a young stellar population. To test the impact of including OB star templates, we generated ∼200 spectra by adding OB star templates. We added 50 per cent host fraction (at 5100 Å) of the total continuum using the OB star template to the spectrum of high luminous AGNs that originally had almost negligible host galaxy and iron contributions. We fitted the simulated spectrum with stellar templates, including and excluding OB star templates from the stellar template list, and found the mean difference to be 16.94 ± 6.62 per cent in this case. This implies that for the young population, our empirical relation may underestimate host galaxy fraction by up to ∼ 17 per cent.We also performed the simulations for two extreme cases by adding 1) a host fraction of 10 per cent that resulted in the host fraction being underestimated by 10.00 ± 9.84 per cent and 2) a host fraction of 80 per cent which gives much higher uncertainty with the host fraction underestimated by 37.75 ± 3.48 per cent, if OB star templates are excluded.

### 3.6 Applications of the empirical relation

We have investigated the applicability of the empirical relation derived in this work (equation (2)), to a completely independent sample having host galaxy measurement from an independent method. We used the sample from Bentz et al. (2013, hereafter, B13). Unlike here, B13 used surface brightness decomposition on the *Hubble Space Telescope* (*HST*) galaxy images and remove the AGN contribution to find the host galaxy from which the starlight contribution could be measured. They used GALFIT (Peng et al. 2002), a non-linear least-squares 2D image fitting algorithm. The host galaxy fraction calculated in B13 is shown with blue-squares in Fig. 6. We use the total luminosity values provided in table 12 and 13 of B13 and calculate the host galaxy fraction using our empirical relation (equation (2)) as shown in red-circles in Fig. 6. We compare these host galaxy fractions and find the mean difference to be 10.5 ± 17.3 per cent. This implies that the empirical relation derived in equation (2), provides acceptable results even for a sample not observed with SDSS.

## 4 SUMMARY

With the advent of large ongoing/upcoming surveys, such as DESI and SDSS, it is important to quantify host galaxy contribution to the AGN spectra in order to reliably estimate black hole mass. In this work, we provide an empirical relation of the host galaxy's stellar luminosity fraction to that of the total luminosity as a function of the total luminosity. For this, we decomposed the host galaxy contribution from AGNs at $z \leq 0.8$ using the optical spectra from SDSS-DR14 with $SNR_{5100} > 10$ leading to 11 415 SDSS spectra and estimated host galaxy fraction by fitting stellar light, AGN power-law continuum and iron blends, simultaneously. The empirical relation obtained from our spectral decomposition method is found to be well-reproducing host-fraction for an independent sample of AGNs where host-fraction was estimated using the image decomposition method. By simulating the spectra at various SNRs, we found the estimated host galaxy fraction to be more reliable for SNR >10. We find that the host galaxy fraction is anticorrelated with the total luminosity and can be well-represented with a 3rd-order polynomial function that can be used to correct the spectrum for host galaxy stellar light contribution to estimate pure AGN continuum luminosity. We found the host galaxy fraction is ≥ 50 per cent for total luminosity of (log $L_{total}$/[erg s$^{-1}$]) ≤ 43.7. A negligible reduction of host galaxy fraction is observed with increasing redshift. The host galaxy fraction is found to be anticorrelated with iron strength and Eddington ratio.

## ACKNOWLEDGEMENTS

We thank the anonymous referee for his/her valuable comments and constructive suggestions which have greatly improved the manuscript. PJ was supported by the Polish National Science Center through grant no. 2020/38/E/ST9/00395. SR acknowledges the partial support of SRG-SERB, DST, New Delhi through SRG grant number SRG/2021/001334.

## DATA AVAILABILITY

The data underlying this article were accessed from SDSS data achieve (https://www.sdss.org/), managed by the Astrophysical Research Consortium for the Participating Institutions of the SDSS-III Collaborations. The derived data generated in this research will be shared upon reasonable request to the corresponding author.

## REFERENCES

Barth A. J. et al., 2015, ApJS, 217, 26
Bentz M. C. et al., 2013, ApJ, 767, 149 (B13)
Berk D. E. V. et al., 2006, ApJ, 131, 84
Bongiorno A. et al., 2014, MNRAS, 443, 2077
Boroson T. A., Green R. F., 1992, ApJS, 80, 109
Calderone G., Nicastro L., Ghisellini G., Dotti M., Sbarrato T., Shankar F., Colpi M., 2017, MNRAS, 472, 4051 (C17)
Cardelli J. A., Clayton G. C., Mathis J. S., 1989, ApJ, 345, 245
Crenshaw D. M., Kraemer S. B., Gabel J. R., 2003, ApJ, 126, 1690
Gkini A., Plionis M., Chira M., Koulouridis E., 2021, A&A, 650, A75
Greene J. E., Ho L. C., 2005, ApJ, 627, 721
Kormendy J., Ho L. C., 2013, ARA&A, 51, 511
Kovačević J., Popović L. Č., Dimitrijević M. S., 2010, ApJS, 189, 15
Madau P., Dickinson M., 2014, ARA&A, 52, 415
Mannucci F., Basile F., Poggianti B. M., Cimatti A., Daddi E., Pozzetti L., Vanzi L., 2001, MNRAS, 326, 745
Markwardt C. B., 2009, in Bohlender D. A., Durand D., Dowler P.eds, ASP Conf. Ser. Vol. 411, Astronomical Data Analysis Software and Systems XVIII. Astron. Soc. Pac., San Francisco, p. 251,

Olguín-Iglesias A., Kotilainen J., Chavushyan V., 2019, MNRAS, 492, 1450
Pâris I. et al., 2018, A&A, 613, A51
Peng C. Y., Ho L. C., Impey C. D., Rix H.-W., 2002, ApJ, 124, 266
Rakshit S., Woo J.-H., 2018, ApJ, 865, 5
Rakshit S., Stalin C. S., Chand H., Zhang X.-G., 2017, ApJS, 229, 39
Rakshit S., Stalin C. S., Kotilainen J., 2020, ApJS, 249, 17 (R20)
Schlegel D. J., Finkbeiner D. P., Davis M., 1998, ApJ, 500, 525
Shen Y. et al., 2011, ApJS, 194, 45
Valdes F., Gupta R., Rose J., Singh H., Bell a., 2008, ApJS, 152, 251
Varisco L., Sbarrato T., Calderone G., Dotti M., 2018, A&A, 618, A127
Woo J.-H., Yoon Y., Park S., Park D., Kim S. C., 2015, ApJ, 801, 38

This paper has been typeset from a TEX/LATEX file prepared by the author.